New Approaches to the Simulation of Heat-Capacity Curves and Phase Diagrams of Pseudobinary Phospholipid Mixtures

Christof Johann, Patrick Garidel, Lutz Mennicke, and Alfred Blume
Fachbereich Chemie, Universität Kaiserslautern, D-67653 Kaiserslautern, Germany

ABSTRACT A simulation program using least-squares minimization was developed to calculate and fit heat capacity (cp) curves to experimental thermograms of dilute aqueous dispersions of phospholipid mixtures determined by high-sensitivity differential scanning calorimetry. We analyzed cp curves and phase diagrams of the pseudobinary aqueous lipid systems 1,2-dimyristoyl-*sn*-glycero-3-phosphatidylglycerol/1,2-dipalmitoyl-*sn*-glycero-3phosphatidylcholine (DMPG/DPPC) and 1,2-dimyristoyl-*sn*-glycero-3-phosphatidic acid/1,2-dipalmitoyl-*sn*-glycero-3-phosphatidylcholine (DMPA/DPPC) at pH 7. The simulation of the cp curves is based on regular solution theory using two nonideality parameters ρ_g and ρ_l for symmetric nonideal mixing in the gel and the liquid-crystalline phases. The broadening of the cp curves owing to limited cooperativity is incorporated into the simulation by convolution of the cp curves calculated for infinite cooperativity with a broadening function derived from a simple two-state transition model with the cooperative unit size $n = \Delta H_{vH}/\Delta H_{cal}$ as an adjustable parameter. The nonideality parameters and the cooperative unit size turn out to be functions of composition. In a second step, phase diagrams were calculated and fitted to the experimental data by use of regular solution theory with four different model assumptions. The best fits were obtained with a four-parameter model based on nonsymmetric, nonideal mixing in both phases. The simulations of the phase diagrams show that the absolute values of the nonideality parameters can be changed in a certain range without large effects on the shape of the phase diagram as long as the difference of the nonideality parameters for ρ_g for the gel and ρ_l for the liquid-crystalline phase remains constant. The miscibility in DMPG/DPPC and DMPA/DPPC mixtures differs remarkably because, for DMPG/DPPC, $\Delta\rho = \rho_l - \rho_g$ is negative, whereas for DMPA/DPPC this difference is positive. For DMPA/DPPC, this difference is interpreted as being caused by a negative ρ_g value, indicating complex formation of unlike molecules in the gel phase.

INTRODUCTION

The phase behavior of phospholipids in water has been studied in great detail, and numerous phase diagrams of binary lipid–water systems as a function of water content have been published and critically evaluated (for reviews see Small, 1986; Cevc and Marsh, 1987; Cevc, 1993; Chernik, 1995). When two different lipids and water are mixed we have to deal with a ternary system. When both lipids and the lipid mixtures form lamellar phases one is particularly interested in the mixing behavior of the two phospholipids in the plane of the bilayer, because this question is relevant to the mixing of different lipids in the bilayer of a biological membrane (Glaser, 1993). The thermotropic behavior of two-component lipid bilayers in excess water is commonly described in terms of a temperature-composition diagram, i.e., a pseudobinary phase diagram. As stated above, in reality we are dealing with a ternary phase diagram in which lamellar phases with different water content are in equilibrium with excess water. During the transition from the low-temperature lamellar phase to the liquid-crystalline lamellar phase, the water content of the lamellar phase changes. In these ternary systems the water content of the lamellar phases is usually not known but is assumed to be similar to the water content in the corresponding binary lipid water systems. The heat effects in the transition region observed by calorimetry originate mainly from changes in intramolecular energy of the fatty acyl chains of the lipids and from changes in intermolecular interactions between the chains, whereas contributions caused by changes in headgroup interactions or by changes in hydration are negligible (see Cevc and Marsh, 1987, and references therein). In an approximation, the ternary system is therefore considered a pseudobinary one, if one neglects the effects caused by changes in water content of the lamellar phases and considers only the mixing behavior of the two lipids within the bilayers of the lamellar phases. When we use the term "binary system" in what follows, we always mean a mixture of two lipids in excess water, using the approximation stated above.

The shape of the pseudobinary phase diagram determined by differential scanning calorimetry depends mainly on the lateral lipid–lipid interactions. In the case of nearly ideal miscibility of two lipids A and B in the bilayers the attractive forces between a molecule of type A and one of type B are approximately the same as between A and A (or B and B). The phase boundaries, i.e., the solidus and liquidus curves, enclose a cigarlike two-phase region in the *T*/*x* diagram. Miscibility gaps will occur if the interactions differ significantly. The extent of deviation from ideal behavior can be expressed in terms of so-called nonideality parame

Received for publication 21 March 1996 and in final form 9 September 1996.

Address reprint requests to Prof. Dr. A. Blume, Fachbereich Chemie der Universität Kaiserslautern, Postfach 3049, D-67653 Kaiserslautern, Germany. Tel.: 49-631-205-2537; Fax: 49-631-205-2187; E-mail: blume@rhrk.uni-kl.de.

0006-3495/96/12/3215/14 $2.00

ters ρ, representing the excess free energies of mixing. A ρ value of zero means that the components are randomly miscible. A positive ρ indicates a tendency to clustering of like molecules, whereas for negative ρ values AB pairs are preferred.

An easy way to obtain experimental data to construct a pseudobinary phase diagram is differential scanning calorimetry (DSC) of dilute aqueous suspensions of multilamellar liposomes of lipid mixtures. The temperatures that correspond to points on the liquidus and solidus curves of the phase diagrams are determined from the experimental heat-capacity curves. One of the main problems that one has to solve is to define the onset and the end temperatures of "melting" ($T(-)$ and $T(+)$, respectively) for every single transition curve in a standardized manner, because of the lack of a theoretically justified method. One way to do this is to take the intersection points between the baseline and the tangents of the ascending and descending parts of the DSC peaks (Inoue et al., 1992); another, which is fraught with a certain arbitrariness, is to determine $T(-)$ and $T(+)$ "by intuitivity" and to correct the width of the transition with the width of the transitions of the pure components, weighted by their mole fractions (Inoue et al., 1992; Nibu et al., 1995; Tenchov, 1985).

To avoid this subjective method we developed a FORTRAN routine that is able to find $T(-)$ and $T(+)$ by simulating the heat-capacity curves that are obtained by DSC, using different thermodynamic approaches for the description of the miscibility of phospholipids. We incorporated the a priori unknown "width" of the phase transition into the model simulation as a variable parameter describing the cooperativity of the transition by using a simple two-state model. We will show that this procedure leads to values of $T(-)$ and $T(+)$ that are different from those obtained with the previously described methods. Additional information on the miscibility properties can be gained from the composition dependence of the nonideality parameter ρ and of the cooperativity parameter. In many cases it was found that the resulting phase diagrams were nonsymmetric, so good simulations of the liquidus and solidus curves of the phase diagrams can be obtained only by use of thermodynamic models for nonsymmetric mixtures.

MATERIALS AND METHODS

DPPC, DMPG, and DMPA were gifts from Nattermann Phospholipid GmbH (Cologne, Germany). The compounds were ≈99% pure as determined by thin-layer chromatography and therefore were used without further purification.

We prepared lipid mixtures in organic solvent by mixing the appropriate volumes of lipids from stock solutions in $CHCl_3$/MeOH (2:1, v:v). The solvent was then evaporated in a stream of argon at higher temperature. The resulting lipid films were dried under high vacuum for 24 h to remove residual traces of solvent. The appropriate excess of ultrapure water (Reinstwassersystem RS 90–4 MF, Barsbüttel, Germany) was added, and the samples were then vigorously vortexed for 5 min at temperatures above T_m of the lipids and additionally for 5 min at room temperature. This procedure leads to a dispersion of multilamellar vesicles in excess water. The pH of the lipid dispersions was checked and adjusted to pH 7.0 with dilute NaOH. The pH was measured before and after the DSC experiments. No changes in pH were observed.

DSC analysis of the thermotropic phase behavior of aqueous pseudobinary lipid dispersions was performed with a MicroCal MC-2 scanning calorimeter (MicroCal, Inc., Amherst, MA) with a heating rate of 1°C/min and lipid concentrations of 0.5–2.5 mg/ml. The reference cell was filled with pure water. As mentioned above, we are actually measuring the transition behavior of a ternary system, which is considered in an approximation to be a pseudobinary one, neglecting changes in water concentration in the lamellar phases. For a check of reproducibility, three scans were usually recorded with each of the three independently prepared samples. The samples were subsequently analyzed by thin-layer chromatography for possible hydrolysis. The accuracy of the transition temperature T_m is ± 0.1°C and that of the transition enthalpies ΔH was ± 0.2 kcal/mol. The experimental data were evaluated with the Origin software package as supplied by MicroCal.

THEORETICAL CALCULATIONS

Calculation of "ideal" heat-capacity curves

First we present a mathematical expression for a heat-capacity curve for binary mixtures with nonideal mixing, representing the hypothetical case of a gel-to-liquid-crystalline (l.c.) phase transition with infinitely high cooperativity (which we call the cp^{id} curve). This kind of function was calculated from experimental phase diagrams by Mabrey and Sturtevant (1976). Because our aim is to calculate heat-capacity curves and phase diagrams for mixtures with nonideal mixing behavior and then fit them to the experimental curves, we need to derive the relevant equations for the calculation of cp^{id} first, using different miscibility models. The effects of limited cooperativity are then introduced in the form of a "cooperativity function," with which the cp^{id} curves are folded.

For a system of two different lamellar phases in equilibrium, neglecting the third phase (excess water), we can write the molar enthalpy as

$$H = \varphi H_g + (1 - \varphi)H_l, \tag{1}$$

with

$$\varphi = \frac{x - x_l}{x_g - x_l}, \tag{2}$$

where H_g and H_l represent the enthalpies of the gel and the l.c. phases, respectively. Because we have no knowledge of the water content of the two different lamellar phases and because the enthalpic effects observed by calorimetry originate mainly from changes in order and in the interactions of the chains, these enthalpies H_g and H_l can be thought of in an approximation as being the enthalpies of the lipid molecules alone. φ is the degree of the phase transition, and the two quantities x_g and x_l are mole fractions of component 2 that describe the composition in the solid and l.c. phases in equilibrium at a given temperature. x is the mole fraction of the whole mixture. H_g and H_l can be written as a sum of enthalpies of the components for 1 and 2 and an excess term

ΔH^E, which is a measure of the deviation of the system from ideal behavior in the gel and the l.c. phases:

$$H_g = (1 - x_g)H_{g1} + x_g H_{g2} + \Delta H_g^E, \quad (3)$$

$$H_l = (1 - x_l)H_{l1} + x_l H_{l2} + \Delta H_l^E. \quad (4)$$

Combination of Eqs. 1–4 gives

$$H = (1 - x)H_{l1} + xH_{l2} - \varphi(1 - x_g)\Delta H_l - \varphi x_g \Delta H_2 + \varphi \Delta H_g^E + (1 - \varphi)\Delta H_l^E, \quad (5)$$

where $\Delta H_1 = H_{l1} - H_{g1}$ and $\Delta H_2 = H_{l2} - H_{g2}$, respectively.

The next step in the calculation depends on the kind of approximation that one is going to choose for the excess enthalpy. Considering the Gibbs–Helmholtz equation for the free excess energy of mixing,

$$\Delta G^E = \Delta H^E - T\Delta S^E, \quad (6)$$

two borderline cases have been postulated. Neither of them occur in real systems because the enthalpy and the entropy of mixing are mutually conditional (Prausnitz et al., 1986): $\Delta S^E = 0$ (case of "regular" mixtures) (Hildebrandt, 1929) and $\Delta H^E = 0$ (case of "athermic" mixtures) (Guggenheim, 1944). In this study we always use $\Delta S^E = 0$, i.e., regular solution theory.

Developing the free excess energy of mixing ΔG^E as a function of the mole fraction x, one obtains

$$\Delta H^E = \Delta G^E = x(1 - x) \cdot [\rho_1 + \rho_2(2x - 1) + \rho_3(2x - 1)^2 + \rho_4(2x - 1)^3 + \ldots], \quad (7)$$

where ρ_1 and $\rho_2, \ldots$ are nonideality parameters that depend on the degree of miscibility (Tenchov, 1985).

Two different sets of equations are chosen to simulate the heat-capacity curves and the phase behavior of the lipid systems DMPG/DPPC and DMPA/DPPC:

1) In the program SIFA we use the approach for symmetric mixtures and assume nonideal mixing in the gel and the l.c. phases:

$$\Delta H_l^E = x_l(1 - x_l)\rho_l \quad (8)$$

and

$$\Delta H_g^E = x_g(1 - x_g)\rho_g. \quad (9)$$

2) In the program ORPHEUS we assume that the gel phase shows nonideal nonsymmetric mixing, whereas the l.c. phase behaves in an ideal way (Tenchov, 1985):

$$\Delta H_g^E = x_g(1 - x_g)[\rho_{g1} + \rho_{g2}(2x_g - 1)], \quad (10)$$

$$\Delta H_l^E = 0. \quad (11)$$

We can evaluate the cp^{id} functions for models 1) and 2), respectively, by inserting Eqs. 8 and 9 (or 10 and 11, respectively) into Eq. 5, using

$$cp^{id} = \left(\frac{\partial H}{\partial T}\right)_P. \quad (12)$$

Considering only terms that contain

$$\left(\frac{\partial x_g}{\partial T}\right), \qquad \left(\frac{\partial x_l}{\partial T}\right),$$

we get two different equations for the cp^{id} function by using the approaches above, namely,

1) Symmetric nonideal mixing in gel and l.c. phases (program SIFA)

$$cp^{id} = h1 + h2 + A + B, \quad (13)$$

with

$$h1 = -(1 - \varphi)\frac{1}{x_g - x_l}(x_g - 1)\Delta H_A\left(\frac{\partial x_l}{\partial T}\right) - \varphi\frac{1}{x_g - x_l}(x_l - 1)\Delta H_A\left(\frac{\partial x_l}{\partial T}\right), \quad (14)$$

$$h2 = (1 - \varphi)\frac{x_g}{x_g - x_l}\Delta H_B\left(\frac{\partial x_l}{\partial T}\right) + \varphi\frac{x_l}{x_g - x_l}\Delta H_B\left(\frac{\partial x_g}{\partial T}\right), \quad (15)$$

$$A = (1 - \varphi)\frac{x}{x_g - x_l}(x_g - 1)\rho_g\left(\frac{\partial x_l}{\partial T}\right) + \varphi\frac{\rho_g(x_g^2 + 2x_g x_l - x_l)}{x_g - x_l}\left(\frac{\partial x_g}{\partial T}\right), \quad (16)$$

$$B = \varphi\frac{1}{x_g - x_l}(1 - x_l)\rho_l\left(\frac{\partial x_g}{\partial T}\right) + (1 - \varphi)\frac{\rho_l(x_l^2 - 2x_g x_l + x_g)}{x_g - x_l}\left(\frac{\partial x_l}{\partial T}\right); \quad (17)$$

2) Nonsymmetric nonideal mixing in the gel and ideal mixing in the l.c. phases (program ORPHEUS):

$$cp^{id} = h1 + h2 + \Psi - \Omega + \Phi + \Gamma, \quad (18)$$

with $h1$ and $h2$ as before (Eqs. 14 and 15) and

$$\Psi = \left(\frac{\partial x_g}{\partial T}\right)\varphi[\rho_{g1} - \rho_{g2} + x_g(6\rho_{g2} - 2\rho_{g1}) - 6x_g^2\rho_{g2}], \quad (19)$$

$$\Omega = \left(\frac{\partial x_g}{\partial T}\right)\varphi \cdot \left[\left(\frac{x_g}{x_g - x_l}\right)(\rho_{g1} - \rho_{g1}x_g + 3\rho_{g2}x_g - 2\rho_{g2}x_g^2 - \rho_{g2})\right], \quad (20)$$

$$\Phi = \left(\frac{\partial x_l}{\partial T}\right)\left(\frac{x_g}{x_g - x_l}\right)[\rho_{g2} - \rho_{g1} + x_g(\rho_{g1} - 3\rho_{g2}) + 2\rho_{g2}x_g^2], \tag{21}$$

$$\Gamma = \left(\frac{\partial x_l}{\partial T}\right)\varphi\left(\frac{x_g}{x_g - x_l}\right)(\rho_{g1} - \rho_{g1}x_g + 3\rho_{g2}x_g - 2\rho_{g2}x_g^2 - \rho_{g2}). \tag{22}$$

For the calculation of the cp^{id} function we need the derivatives of the mole fractions with respect to the temperature T. We obtain these derivatives from the simulation of the solidus and the liquidus curves of the phase diagram by using the same mixing model and the corresponding nonideality parameters. For symmetric mixtures (SIFA) the following two transcendental equations describe the temperature T for which the two phases with composition x_g and x_l are in equilibrium. These equations are based on the Bragg–Williams approximation (see Hill (1960) and Tenchov (1985) for further details):

$$T = \frac{\Delta H_2 + \rho_l(1 - x_l)^2 - \rho_g(1 - x_g)^2}{(\Delta H_2/T_2) - R\ln(x_l/x_g)}, \tag{23}$$

$$T = \frac{\Delta H_1 + \rho_l x_l^2 - \rho_g x_g^2}{(\Delta H_1/T_1) - R\ln[(1 - x_l)/(1 - x_g)]}. \tag{24}$$

ΔH_1, ΔH_2 and T_1, T_2 represent the transition heat and temperature of components 1 and 2, respectively. To obtain x_g and x_l and their derivatives with respect to T as a function of temperature we have to solve these two equations, using iterative procedures.

For the model with nonsymmetric nonideal mixing in the gel phase and ideal mixing in the l.c. phase (program ORPHEUS) the respective expressions are

$$T = \frac{\Delta H_2 - (1 - x_g)^2[\rho_{g1} + \rho_{g2}(4x_g - 3)]}{(\Delta H_2/T_2) - R\ln(x_l/x_g)}, \tag{25}$$

$$T = \frac{\Delta H_1 - x_g^2[\rho_{g1} + \rho_{g2}(4x_g - 1)]}{(\Delta H_1/T_1) - R\ln[(1 - x_l)/(1 - x_g)]}. \tag{26}$$

The resulting cp^{id} functions have shapes similar to those calculated by Mabrey and Sturtevant (1976). They cannot be fitted to the experimental heat-capacity curves because they have been derived with the assumption of infinite cooperativity, i.e., the assumption that lipids show a true first-order phase transition.

For lipid bilayer systems it is known that even in highly purified pure lipids the transition is of finite width. The simplest way to consider this effect in a first approximation is to introduce a broadening function based on a simple two-state model. This model takes only two different lipid states into account, namely, an ordered lipid (gel phase) and a l.c. lipid (Blume, 1988). Of course, this is a simplification of the real situation, because in reality we are dealing with a transition in which the water content of the lamellar phases changes, i.e., water molecules take part in the transition from the ordered to the disordered lamellar state (Chernik, 1995). Whatever the real situation is, the transitions in systems with two lipids in water are additionally broadened by a decrease in cooperativity. We can show this by measuring the width of the transition as a function of vesicle size in unilamellar lipid vesicles (Gruenewald et al., 1979). The cooperativity in vesicles is strongly decreased because of curvature strain. In lipid mixutures one would expect a further decrease in cooperativity owing to a steric mismatch of the two lipid molecules in the bilayers. In what follows, we describe how we use this broadening function to obtain better fits for the heat-capacity curves.

Calculation of the broadening function

Using the approximations stated above, i.e., assuming that the participation of water in the transition can be neglected, we have an equilibrium between a gel-phase lipid S and a l.c. lipid L of the form

$$S \rightleftharpoons L. \tag{27}$$

Assuming that lipid molecules form domains of constant size (Tenchov, 1985) that do not interact, one can define an equilibrium constant K:

$$K = \frac{[L]}{[S]} = \frac{1 - \Theta}{\Theta}. \tag{28}$$

S and L represent the number of lipids in the gel and the l.c. phases, respectively, and Θ is the degree of the transition running from 1 (all lipids in the gel state) to 0 (all lipids in the l.c. state).

With the van't Hoff equation

$$\left(\frac{\partial \ln K}{\partial T}\right)_p = \frac{\Delta H_{vH}}{RT^2}, \tag{29}$$

one obtains

$$\left(\frac{-1}{1 - \Theta} - \frac{1}{\Theta}\right)\left(\frac{\partial \Theta}{\partial T}\right) = \frac{\Delta H_{vH}}{RT^2}, \tag{30}$$

$$\Theta(T) = \left\{1 + \exp\left[\frac{-\Delta H_{vH}}{R}\left(\frac{1}{T} - \frac{1}{T_m}\right)\right]\right\}^{-1}, \tag{31}$$

$$\frac{\partial \Theta}{\partial T} = \frac{\exp[-(\Delta H_{vH}/R)(1/T - 1/T_m)]\Delta H_{vH}/RT^2}{\{1 + \exp[-(\Delta H_{vH}/R)(1/T - 1/T_m)]\}^2}. \tag{32}$$

The higher ΔH_{vH}, the so-called van't Hoff transition enthalpy, is, the higher is the cooperativity of the transition. For ΔH_{vH} approaching infinity we have the case of infinitely high cooperativity, i.e., a true first-order phase transition.

To simulate the experimental data for the heat-capacity curves we convoluted the cp^{id} curves (see Eqs. 13 and 18) with the broadening function described by Eq. 32 to obtain a new heat-capacity curve, which we call cp^{sim}:

$$cp^{sim} = \left(\frac{\partial \Theta}{\partial T}\right) \otimes cp^{id}. \tag{33}$$

The simplest way to perform the convolution is to multiply the two functions in Fourier space rather than to perform the calculation of the convolution integral directly. Both functions are separately Fourier transformed and then multiplied, and the resulting function is then backtransformed to yield the cp^{sim} curve.

With the equations derived above we have now developed the desired computer programs. The flow chart in Fig. 1 shows the essential steps. For the variation of the nonideality parameters and ΔH_{vH} we used the Simplex algorithm (Press et al., 1986); we calculate the goodness of fit by using the least-squares method (Faunt and Johnson, 1992).

Once the heat-capacity curves have been fitted, one obtains the values of the nonideality parameters and in that way can calculate $T(-)$ and $T(+)$ from Eqs. 23 and 24 for symmetric nonideal mixtures (SIFA) or from Eqs. 25 and 26 for nonsymmetric nonideal mixing only in the gel phase (ORPHEUS). From these $T(-)$ and $T(+)$ values the phase diagram that is based on the assumption of true first-order phase transitions can now be constructed.

We show that the simulations of the different experimental heat-capacity curves lead to values of the nonideality parameters that depend on the composition of the mixtures. It is therefore advisable for an independent check to simulate the phase diagrams again with different mixing models.

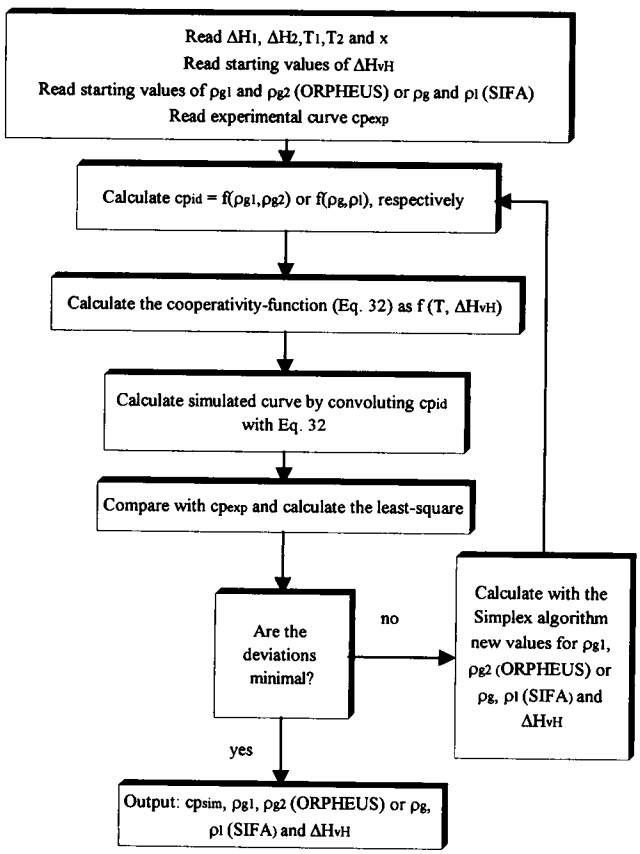

FIGURE 1 Flow chart of the programs SIFA and ORPHEUS used to simulate heat-capacity curves of binary lipid mixtures obtained by DSC.

Simulation of phase diagrams

Phase diagrams of pseudobinary lipid systems have already been simulated by a number of researchers, e.g., by Lee (1977), van Dreele (1978), and Cheng (1980) with a quasi-chemical approach; by Ipsen and Mouritsen (1988) with a regular solution theory with one adjustable parameter; and by Brumbaugh et al. (1990), Brumbaugh and Huang (1992), and Tenchov (1985) with Eqs. 23 and 24, which are based on the assumption of symmetric mixtures described by Eqs. 8 and 9.

Brumbaugh et al. (1990) achieved good fits to the experimental phase diagrams; they obtained the $T(-)$ and $T(+)$ values in the standard way by varying the nonideality parameters and additionally the transition temperatures T_m and enthalpies ΔH_{cal} of the pure lipids. In our opinion these parameters should be kept fixed. Consequently we varied only the nonideality parameters ρ_g and ρ_l for the fits to our $T(-)$ and $T(+)$ values obtained in a different way, i.e., by direct simulation of the heat-capacity curves by removing the additional broadening by the limited cooperativity of the transition.

Overall we used four different models for the simulation of phase diagrams; two of those, models I and IV, are based on equations described above, and the other two are more complicated and are described below.

Model I

Model I is based on Eqs. 23 and 24. It is the model for nonideal symmetric mixing in the gel and l.c. phases.

Model II

For model II we assume symmetric nonideal mixing and, additionally, that the nonideality depends linearly on temperature. The expression for the excess free energy of mixing ΔG^E is then

$$\Delta G^E = \Delta H^E - T\Delta S^E = x(1-x)(\rho_1 + \rho_2 T) = x(1-x)\rho_1 + x(1-x)T\rho_2, \quad (34)$$

with

$$\Delta H^E = x(1-x)\rho_1, \quad (35)$$

$$\Delta S^E = -x(1-x)\rho_2. \quad (36)$$

Unlike in all other models presented here, the excess entropy of mixing ΔS^E here is not zero.

The calculation of the equations for coexistence is performed in the usual way on the basis of the expressions for the excess quantities of the chemical potential μ^E for the two phases (g and l) by use of the Bragg–Williams theory (Lee, 1977; Tenchov, 1985). The two resulting equations are

$$T = \frac{\Delta H_l + \rho_{l1}x_l^2 - \rho_{g1}x_g^2}{(\Delta H_l/T_l) - R\ln[(1-x_l)/(1-x_g)] - x_l^2\rho_{l2} + x_g^2\rho_{g2}}, \quad (37)$$

$$T = \frac{\Delta H_2 + \rho_{l1}(1 - x_l)^2 - \rho_{g1}(1 - x_g)^2}{(\Delta H_2/T_2) - R \ln(x_l/x_g) - (1 - x_l)^2\rho_{l2} + (1 - x_g)^2\rho_{g2}}. \quad (38)$$

Model III

Model III uses nonideal and nonsymmetric mixing behavior for gel and l.c. phases, respectively:

$$\Delta H_g^E = x_g(1 - x_g)[\rho_{g1} + \rho_{g2}(2x_g - 1)], \quad (39)$$

$$\Delta H_l^E = x_l(1 - x_l)[\rho_{l1} + \rho_{l2}(2x_l - 1)]. \quad (40)$$

The equations for coexistence are

$$T = \frac{\Delta H_2 + (1 - x_l)^2[\rho_{l1} + \rho_{l2}(4x_l - 1)] - (1 - x_g)^2[\rho_{g1} + \rho_{g2}(4x_g - 1)]}{(\Delta H_2/T_2) - R \ln(x_l/x_g)}, \quad (41)$$

$$T = \frac{\Delta H_1 + x_l^2[\rho_{l1} + \rho_{l2}(4x_l - 3)] - x_g^2[\rho_{g1} + \rho_{g2}(4x_g - 3)]}{(\Delta H_1/T_1) - R \ln[(1 - x_l)/(1 - x_g)]}. \quad (42)$$

Model IV

Model IV was described above. It assumes ideal mixing behavior in the l.c. phase and nonideal nonsymmetric mixing behavior in the gel phase. We use Eqs. 10 and 11 and the equations of coexistence 25 and 26.

Simulation strategy

A computer program called FASE is used to simulate and adjust a solidus and a liquidus curve to the $T(-)$ and $T(+)$ values that have been obtained with SIFA or ORPHEUS; the strategy of the algorithm is almost the same as described elsewhere (Brumbaugh and Huang, 1992).

Given the starting values of the nonideality parameters (and also the transition enthalpies and temperatures of the pure components), the program fixes x_s (or x_l) in steps of $\Delta x = 0.005$, and for each step the value of x_l or x_s, respectively, is calculated by an iterative procedure by use of the appropriate equations for coexistence. The iteration routine runs 199 times until a specified tolerance (10^{-7}) of the temperature values T is obtained. One obtains a simulated phase diagram, which is then compared with the given $T(-)$ and $T(+)$ values by least-squares methods. New nonideality parameters are generated with the aid of the Simplex algorithm, and the procedure continues until the deviation between theoretical and experimental data is minimal. The flow chart that corresponds to that process is shown in Fig. 2.

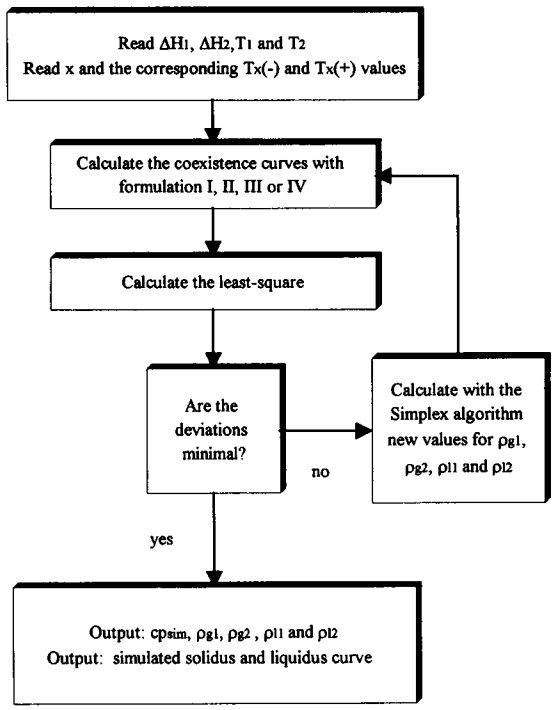

FIGURE 2 Flow chart of the program FASE used to simulate phase diagrams of binary lipid mixtures on the basis of four different thermodynamic formulations for the mixing behavior.

RESULTS AND DISCUSSION

Simulation of heat-capacity curves and comparison with experimental data

The simulation programs SIFA, ORPHEUS, and FASE have been used extensively to examine pseudobinary lipid mixtures of phospholipids with different headgroups and acyl chain structures (P. Garidel, C. Johann, L. Mennicke, and A. Blume, unpublished results). For lipid mixtures with charged lipids we also investigated the effect of pH on the miscibility properties. Here we introduce two examples for lipid mixtures, namely, the systems DMPG/DPPC and DMPA/DPPC at pH 7, to show the possibilities and limitations of the new simulation procedures.

The experimentally obtained DSC curves for these pseudobinary mixtures are shown in Figs. 3 and 4. The pretransitions that are present for the pure lipids and the lipid mixtures are neglected. We analyze only the gel-to-l.c. phase transition. Whereas the data of Fig. 3 for the DMPG/DPPC mixture indicate almost ideal mixing behavior, the curves in Fig. 4 for the system DMPA/DPPC show a higher degree of nonideality because the transition temperature does not decrease linearly with the mole fraction of DPPC.

Both SIFA (symmetric, nonideal mixing in both phases) and ORPHEUS (nonsymmetric, nonideal mixing only in gel phase) have been applied to simulate the heat-capacity curves; the fits obtained with SIFA are shown as dashed curves in Figs. 3 and 4. One can see that the correspondence between calculated and experimental curves is better for the DMPG/DPPC mixture. A comparison of the results of the two simulation programs shows that for DMPG/DPPC and DMPA/DPPC the two simulation models lead to nearly the same results; the differences between the $T(-)$ and $T(+)$ values determined with the two programs are smaller than 1°. Therefore, only the data of SIFA are shown in the figures.

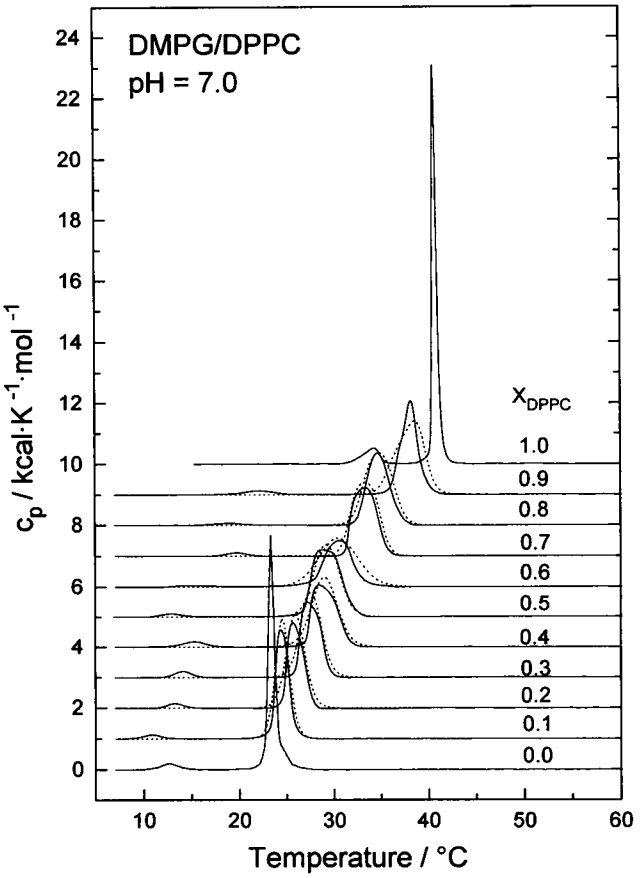

FIGURE 3 DSC curves of mixtures of the system DMPG/DPPC at pH7 (*solid curves*) and the corresponding numerical simulations obtained with SIFA (*dashed curves*).

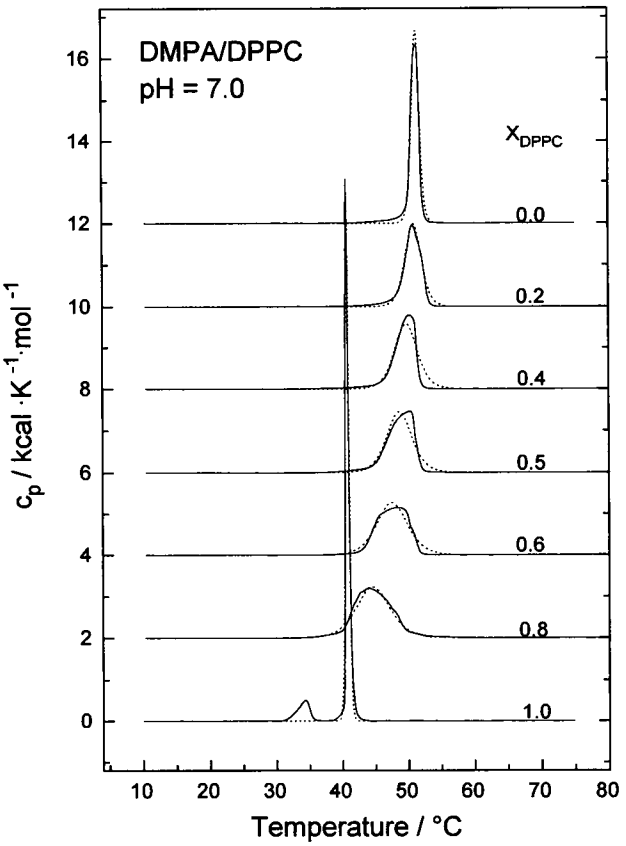

FIGURE 4 DSC curves of mixtures of the system DMPA/DPPC at pH7 (*solid curves*) and the corresponding numerical simulations obtained with SIFA (*dashed curves*).

With the present data one is now able to construct the *T/x* phase diagram in two different ways, as shown in Figs. 5 and 6, for both systems: The filled triangles represent the empirical $T(-)$ and $T(+)$ values obtained by determining the temperatures for onset and end of "melting" in the usual way, namely, from the deviations of the experimental DSC curves from the baseline, correcting them for the width of the transition of the pure compounds weighted with the mole fraction (Mabrey and Sturtevant, 1976). The open circles show the onset ($T-$) and the end ($T+$) temperatures obtained from the simulation with SIFA. For the system DMPG/DPPC the temperatures of these two procedures are nearly identical. However, for the system DMPA/DPPC they differ considerably, the temperature range for the transition being significantly broader when the empirical $T(-)$ and $T(+)$ values are taken.

The explanation for these differences is obvious. The empirical onset and end temperatures (filled triangles) are obtained by correcting only for the limited cooperativity of the transition of the pure lipids weighted with their mole fraction; i.e. a linear behavior of the cooperativity is considered. This means that the cooperativity in a mixture cannot be smaller than that of the individual components. A strong decrease in cooperativity owing to nonideal mixing is not taken into account. This limitation is not present if the degree of cooperativity is a variable parameter, as is the case for simulations with SIFA. This decrease in cooperativity is more pronounced in systems with greater deviations from ideality and has a large influence on the determination of the $T(-)$ and $T(+)$ values in phase diagrams of binary mixtures for which the transition temperatures of the two components are close together, as in the case of DMPA/DPPC. An example of these differences is shown in Fig. 7 for a DMPA/DPPC mixture with $x_{DPPC} = 0.8$. The onset and the end of "melting" temperatures are indicated by arrows in the cp^{id} and the cp^{exp} curves. The $T(-)$ and $T(+)$ values obtained from the simulations are much closer than those obtained by the usual empirical procedure. This example also shows that the fit of the experimental curves is not perfect. One reason for the deviations is that the cp^{id} curve can be folded only with a broadening function of constant width. In reality, the cooperative unit size is probably a function of temperature, so the broadening is much more complicated than assumed in the present model (see below).

The size of the cooperative unit n can be calculated from the ratio of the van't Hoff enthalpy ΔH_{vH} (which one obtains by fitting in the simulation process (see Eq. 31)) and

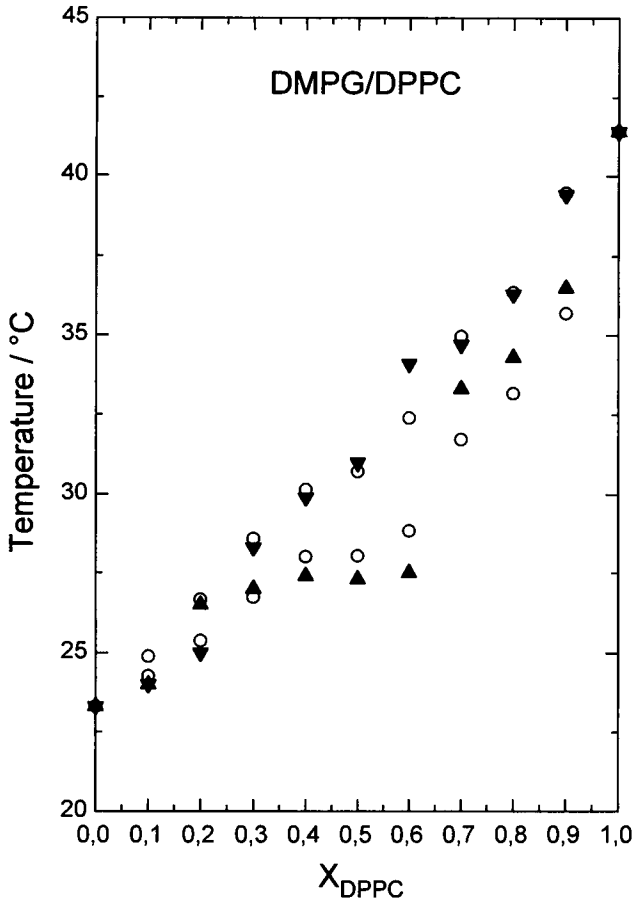

FIGURE 5 Temperatures of onset [$T(-)$] and end [$T(+)$] of "melting" of DMPG/DPPC mixtures obtained (▲) by the usual empirical procedure and (○) from simulations using SIFA.

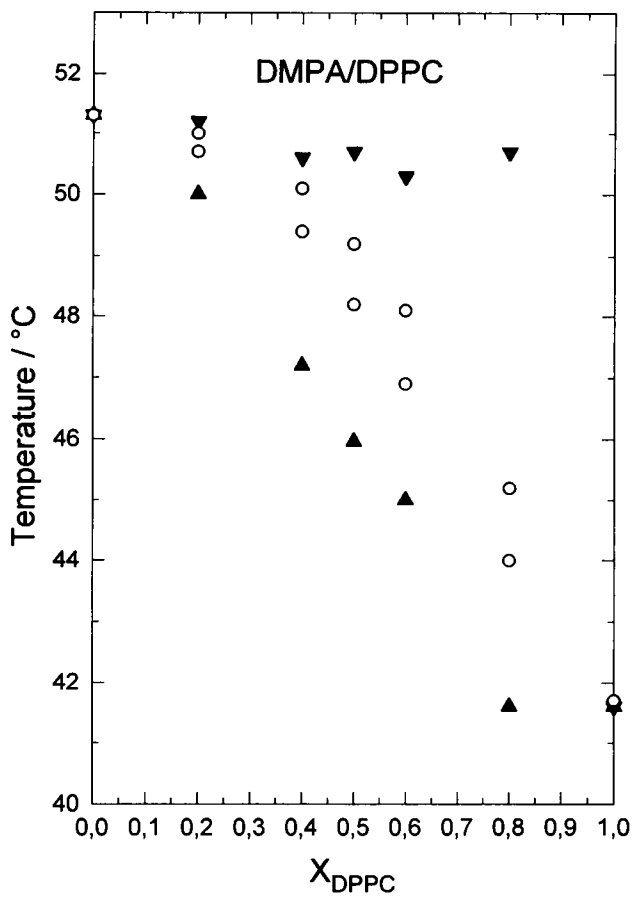

FIGURE 6 Temperatures of onset [$T(-)$] and end [$T(+)$] of "melting" of DMPA/DPPC mixtures obtained by (▲) the usual empirical procedure and (○) from simulations using SIFA.

the experimental transition enthalpy ΔH_{cal}:

$$n = \Delta H_{vH}/\Delta H_{cal}. \quad (43)$$

The advantage of simulating the DSC curves with SIFA or ORPHEUS is now that it is possible to obtain n as a function of mole fraction x. It is obvious that these values are only crude estimates for the cooperative thermotropic behavior of the lipids because of their implicit simplifying assumptions (constant domain size, absence of domain–domain interactions; see Tenchov (1985)). However, they illustrate the correct tendency of the mixtures at different mole fractions. Fig. 8 shows such an n/x plot for the two systems DMPG/DPPC and DMPA/DPPC for which the values for n were obtained from simulations with SIFA. We found the typical U-like shape for many binary lipid systems when we used both SIFA and ORPHEUS. This kind of curve illustrates that the greatest deviations from linear behavior of the cooperativity parameter occur at a mole fraction of ~0.5.

Sugár has presented calculations for the cooperative behavior as a function of temperature and mole fraction for the pseudobinary lipid mixture DMPC/DSPC (Sugár, 1987). These calculations show two effects: the cooperative unit (c.u.) size for a mixture with a given composition is a function of temperature or degree of transition of the mixture. This temperature dependence is particularly large for mixtures with less than 20 mol% of the other component. In our simulations we could convolute the calculated heat-capacity curve only with a broadening function that has a fixed, i.e., temperature independent, c.u. size. For mixtures with more than 20 mol% of the other component these values for c.u. do not differ significantly from the c.u. sizes at the midpoint of the phase transition. The n/x curves in Fig. 8 show qualitatively similar behavior to the calculated curves of Sugár for the DMPC/DSPC mixture; that is, the c.u. size drops significantly at mole fractions between 0.2 and 0.8. Even the absolute values of $n \approx 20$–30 for our systems are not much larger than those for the relatively nonideal DMPC/DSPC mixture of $n \approx 10$. Therefore, the approach of using a fixed value of n does give reasonable results, at least for mixtures in the range $0.2 < x < 0.8$. An asymmetric broadening of the heat-capacity curves owing to the temperature dependence of n would probably give better fits. However, because no a priori knowledge of the temperature dependence of the c.u. unit size exists, this would

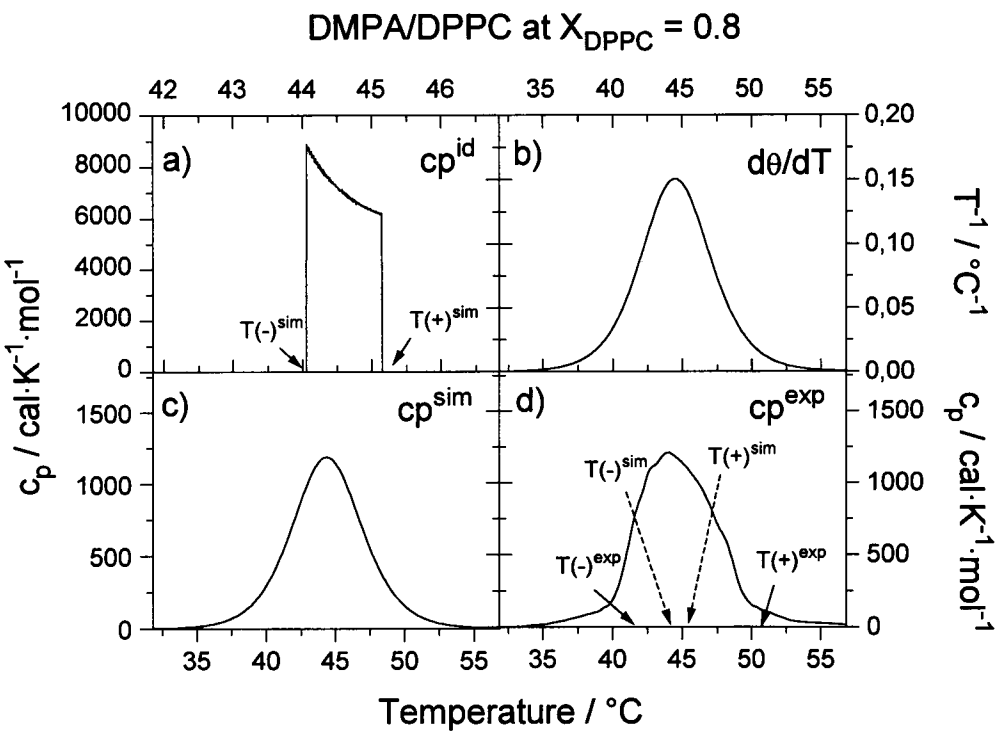

FIGURE 7 Example for determining the $T(-)$ and $T(+)$ values for a DMPA/DPPC mixture with x_{DPPC} = 0.8: (*a*) theoretical cp^{id} curve, where arrows indicate $T(-)$ and $T(+)$ values; (*b*) broadening function with the cooperative unit size n determining the width of the transition; (*c*) cp^{sim} curve obtained after convolution; (*d*) experimental heat-capacity curve, where solid arrows indicate the corrected $T(-)$ and $T(+)$ values obtained empirically and dashed arrows indicate the theoretical onset and end temperatures also shown in (*a*).

introduce new adjustable parameters and increase the calculation time considerably.

Simulation of *T/x* diagrams (phase diagrams) and analysis of the nonideality parameters

Direct simulation of the DSC curves yields not only values for the c.u. size n but also the nonideality parameters as a function of composition. We found that these parameters change with the composition of the mixture. This means that the implicit assumption of a symmetric nonideal mixture (SIFA) is not warranted. The nonideality parameters for the two mixtures as a function of x_{DPPC} are shown in Table 1.

If the nonideality parameters are indeed a function of composition, then this should be apparent from a simulation of the phase diagram by an approach with nonsymmetric nonideal mixtures. We have therefore simulated the phase diagrams, considering the $T(-)$ and $T(+)$ data obtained with SIFA and using the program FASE on the basis of the models I–IV, as mentioned above. These simulations are shown for DMPG/DPPC in Fig. 9 and for DMPA/DPPC in Fig. 10, with the calculated phase diagrams for ideal mixing indicated as dashed curves. The figures show that all four model calculations seem to give acceptable fits to the experimental values, but closer inspection leads to the conclusion that in case of DMPG/DPPC models III and IV that use the approach of nonsymmetric mixtures give better fits, the four-parameter model III being definitely the best. Models I and II give similar fits for DMPG/DPPC, leading to the conclusion that the temperature dependence of the nonideality parameters is low for this mixture. For DMPA/DPPC model I (symmetric nonideal mixing) and model III (non

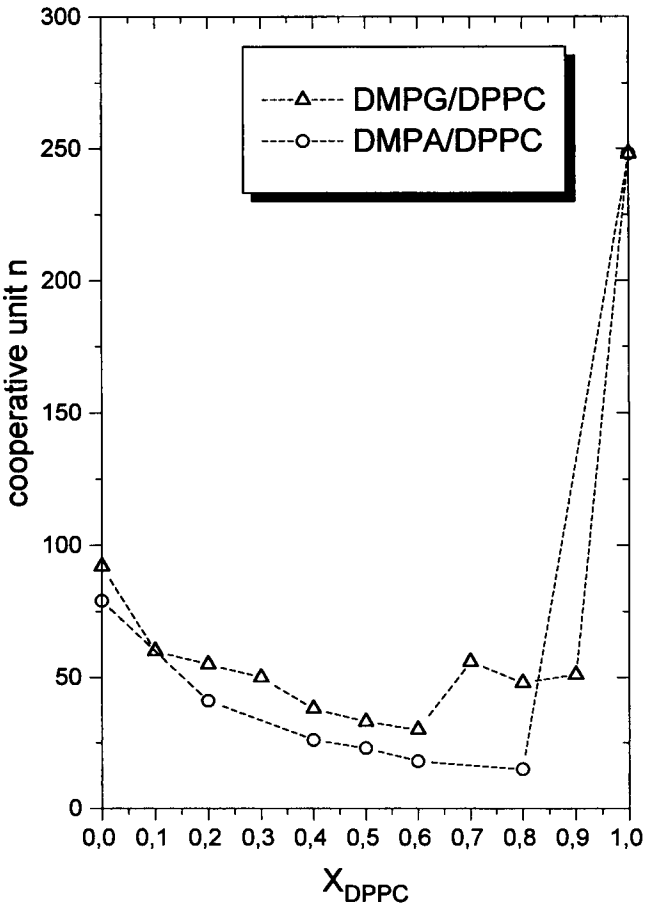

FIGURE 8 Cooperative unit size $n = \Delta H_{vH}/\Delta H_{cal}$ as a function of composition for DMPG/DPPC and DMPA/DPPC as obtained from the simulations of the heat-capacity curves using SIFA.

TABLE 1 Nonideality parameters (in cal/mol) obtained with SIFA from the simulations of the heat-capacity curves using the two-parameter model I

	DMPG/DPPC			DMPA/DPPC		
x_{DPPC}	ρ_g	ρ_l	$\Delta\rho = \rho_l - \rho_g$	ρ_g	ρ_l	$\Delta\rho = \rho_l - \rho_g$
0.1	−172	−410	−238			
0.2	−160	−396	−236	−455	−262	193
0.3	−307	−529	−222			
0.4	−418	−665	−247	−340	−82	258
0.5	−317	−728	−411	−323	−65	258
0.6	−293	−790	−497	−382	−124	258
0.7	−674	−1100	−426			
0.8	−1627	−2233	−606	−290	−58	232
0.9	−148	−721	−573			

symmetric nonideal mixing in both phases) give almost identical fits, model III again being slightly better. The different quality of the fits discussed here is supported by the least-squares deviations. Because model III gives the best fits in both cases we will consider only this model in the further discussion.

For DMPG/DPPC the corrected $T(-)$ and $T(+)$ values and those obtained from the simulations using SIFA are nearly identical (see Fig. 3). For DMPA/DPPC the differences are more significant (see Fig. 4). In this case the $T(-)$ and $T(+)$ values from the simulations lead to an approximately ideal phase behavior. This is illustrated in Fig. 11. Fitting the coexistence lines to the empirically corrected experimental temperatures yields a very broad coexistence range and a phase diagram with an upper azeotropic point at $x_{DPPC} \approx 0.1$, whereas the phase diagram obtained by the new procedure indicates more nearly ideal behavior.

An analysis of the nonideality parameters of the systems is of particular interest. These parameters differ from those that were used in earlier publications (Brumbaugh et al., 1990; Brumbaugh and Huang, 1992; Tenchov, 1985) insofar as they depend on the mole fraction of the mixture. The nonideality parameters obtained from fitting the coexistence lines to the experimentally corrected temperatures and those obtained from the simulations are shown in Table 2. It is immediately evident that the nonideality parameters obtained from the simulations of the complete phase diagram are quite different from those obtained from the simulations of the heat-capacity curves as shown in Table 1. Several reasons can be found for these observations. In the simulations of the heat-capacity curves a two-parameter model using symmetric nonideal mixtures was employed. For the determination of the heat-capacity curves it is necessary to calculate not the complete phase diagram but only the

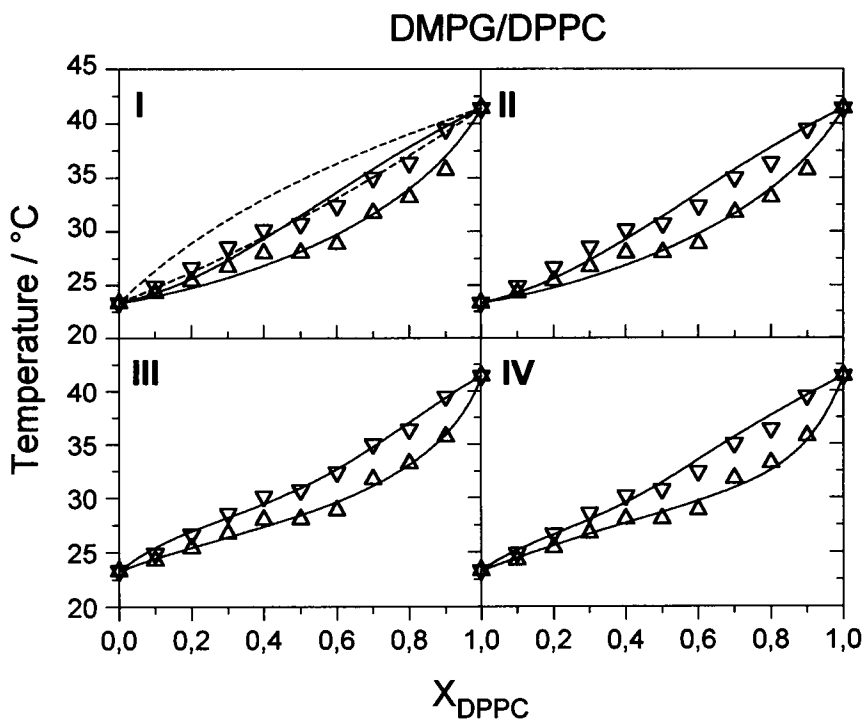

FIGURE 9 Simulation of phase diagrams for DMPG/DPPC on the basis of the $T(-)$ and $T(+)$ temperatures determined by SIFA by use of four different thermodynamic models, I–IV, as described in the text. The dashed curves in diagram I represent the solidus and liquidus curves of the ideal phase diagram.

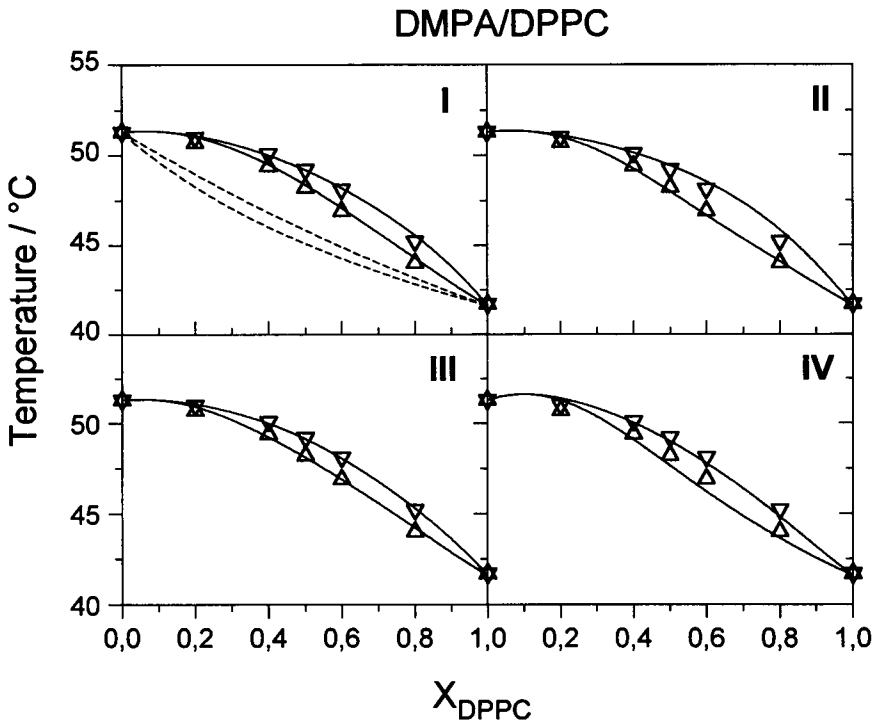

FIGURE 10 Simulation of phase diagrams for DMPA/DPPC on the basis of the $T(-)$ and $T(+)$ temperatures determined by SIFA by use of four different thermodynamic models, I–IV, as described in the text. The dashed curves in diagram I represent the solidus and liquidus curves of the ideal phase diagram.

coexistence lines in the temperature range that covers the transition of the mixture with the specific composition. Therefore each heat-capacity curve contains only information on the sections of the coexistence lines with temperatures inside the transition region. The simulations of heat-capacity curves of mixtures with different compositions then show that the two-parameter model does not fit because the nonideality parameters depend on composition (see above). Therefore, the absolute ρ values cannot be expected to be identical to those obtained from a simulation of a complete phase diagram. In addition, the position and the curvature of the phase boundaries do not change significantly when the ρ values are changed, as long as the differences in the nonideality parameters between l.c. and gel phases remain constant. This has been shown by model calculations of Brumbaugh and Huang (1992) for a variety of parameter sets. For both mixtures example calculations demonstrating this effect are shown in Fig. 12. For DMPG/DPPC the ρ_{g1} values are 0, 200, and 400 cal/mol; the ρ_{l1} values are -350, -150, and $+50$ cal/mol, the difference being constant; whereas the ρ_{g2} and ρ_{l2} values are kept constant at -200 and -450 cal/mol, respectively. Similarly, for DMPA/DPPC the ρ_{g1} values are varied from -300 to $+100$ cal/mol and the ρ_{l1} values from 0 to $+400$ cal/mol, with fixed ρ_{g2} and ρ_{l2} values at -300 and -350 cal/mol, respectively. The shape of the phase diagrams changes only marginally, as predicted. Therefore, the absolute values of the nonideality parameters have large uncertainties, and only the differences between these values for the gel and l.c. phases are reliable parameters that describe the phase diagram.

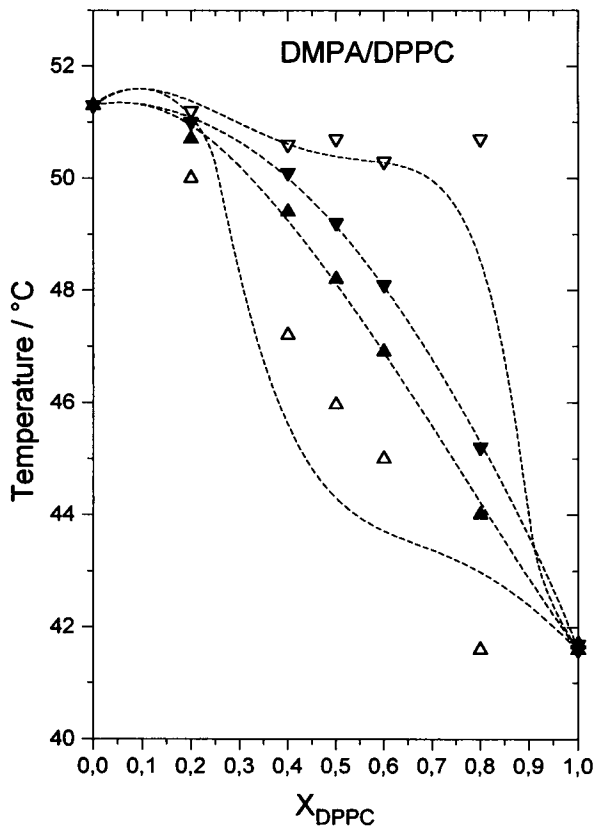

FIGURE 11 Simulations of the DMPA/DPPC phase diagrams (*dashed curves*) on the basis of $T(-)$ and $T(+)$ values determined (▲) by SIFA and (△) on the basis of empirically corrected temperature values. The latter temperature values led to a much broader coexistence range and to a calculated phase diagram with upper azeotropic point at $x_{DPPC} = 0.1$.

TABLE 2 Nonideality parameters (in cal/mol) obtained from the simulations of the phase diagrams on the basis of the empirically corrected experimental $T(-)$ and $T(+)$ values (ρ_{exp} values) and on the basis of the $T(-)$ and $T(+)$ values determined by SIFA using the program FASE with the four-parameter model III (ρ_{sim} values)

	DMPG/DPPC		DMPA/DPPC	
	ρ_{exp}	ρ_{sim}	ρ_{exp}	ρ_{sim}
ρ_{g1}	78	398	990	−270
ρ_{l1}	−281	25	1229	−8
ρ_{g2}	−388	−130	259	−285
ρ_{l2}	−456	−405	124	−325

We have therefore analyzed these differences and plotted them in Fig. 13 as a function of mole fraction. The circles and squares are $\Delta\rho = \rho_l - \rho_g$, obtained from simulations of the heat-capacity curves (data of Table 1); we calculated the curves with the nonideality parameters obtained from the simulation of the phase diagram with FASE, using model III (data of Table 2) with

$$\Delta\rho(x) = \Delta\rho_1 + (2x - 1)\Delta\rho_2. \quad (44)$$

and $\Delta\rho_1 = \rho_{l1} - \rho_{g1}$ and $\Delta\rho_2 = \rho_{l2} - \rho_{g2}$.

Even if the absolute values of the nonideality parameters in the gel or the l.c. phase obtained by the two methods differ strongly, the data sets for $\Delta\rho$ agree remarkably well for both mixtures. As mentioned above, this so because for a certain range of ρ values only $\Delta\rho$ is important for the shape of a phase diagram. For the least-squares method used for fitting the coexistence lines there exist multiple parameter pairs with almost identical minimal values for the least-squares sum with constant $\rho_l - \rho_g$.

The mixtures DMPG/DPPC and DMPA/DPPC have two properties in common: They are mixtures of an uncharged with a negatively charged component, and the chain length differences are two CH_2 groups. The fact that DMPG and DMPA are singly charged at pH 7 is apparently the reason for their nonsymmetric mixing behavior, because electrostatic effects are expected to depend on the surface charge density, which in turn depends on the mole fraction of the charged component. But electrostatic effects cannot be viewed in isolation because they are combined with hydration and hydrogen-bonding effects. This is obviously the reason that the mixing behavior in the gel and the l.c. phases differs in a remarkable way. For DMPG/DPPC the $\Delta\rho$ values are negative, whereas for DMPA/DPPC they are positive. Because of the difficulties in determination of

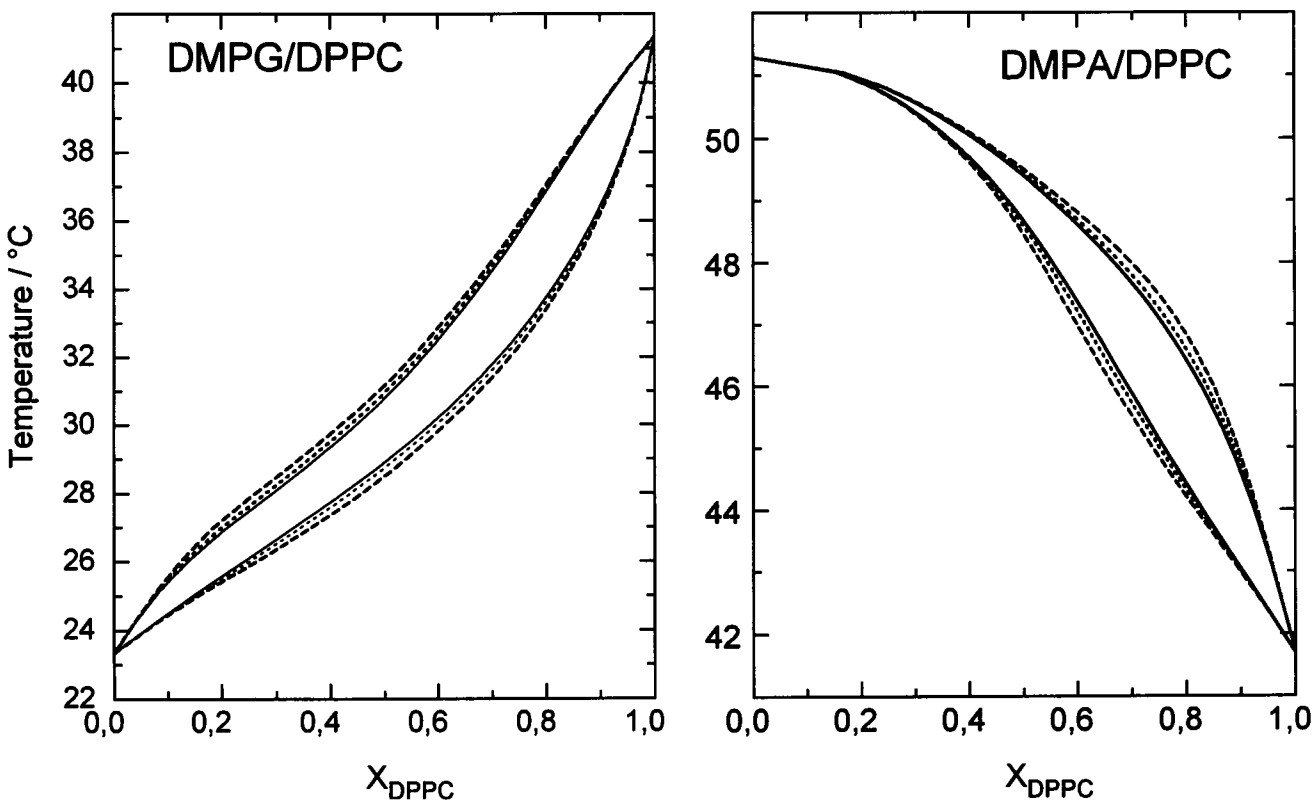

FIGURE 12 Model calculations for phase diagrams with three different parameter sets for the nonideality parameters with constant differences between the ρ values. The following parameter pairs were used: for DMPG/DPPC ρ_{g1}, ρ_{l1} = 0, −350 cal/mol (*solid curves*); ρ_{g1}, ρ_{l1} = +200, −150 cal/mol (*dotted curves*), ρ_{g1}, ρ_{l1} = +400, +50 cal/mol (*dashed curves*); the values for ρ_{g2} and ρ_{l2} were −200 and −450 cal/mol, respectively; for DMPA/DPPC ρ_{g1}, ρ_{l1} = −300, 0 cal/mol (*solid curves*); ρ_{g1}, ρ_{l1} = −100, +200 cal/mol (*dotted curves*); ρ_{g1}, ρ_{l1} = +100, +400 cal/mol (*dashed curves*); the values for ρ_{g2} and ρ_{l2} were −300 and −350 cal/mol, respectively.

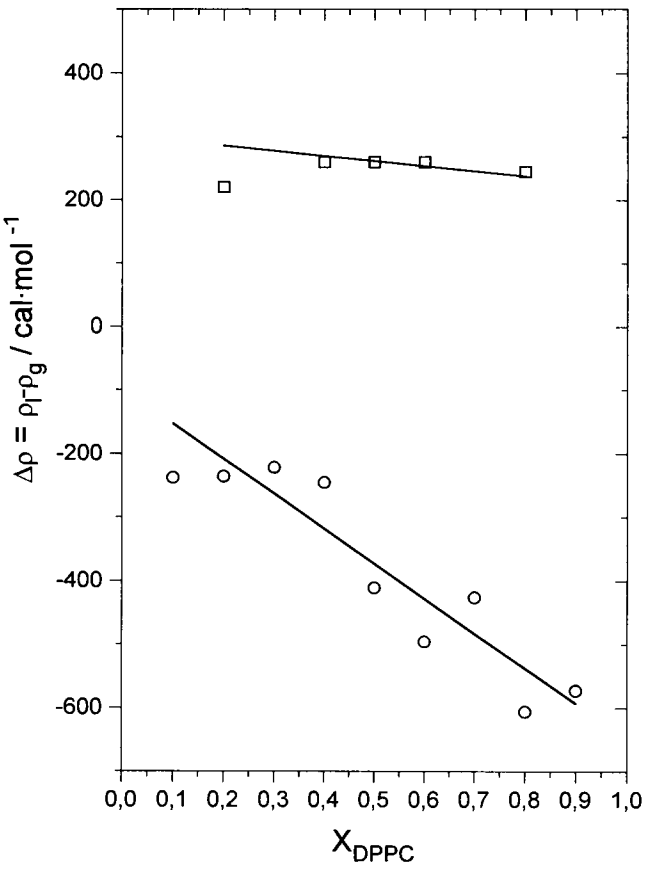

FIGURE 13 Difference in nonideality parameters $\Delta\rho = \rho_l - \rho_g$ obtained with SIFA from the simulations of the individual heat-capacity curves: (○) DMPG/DPPC, (□) DMPA/DPPC (data from Table 1). The curves were calculated from the nonideality parameters shown in Table 2 as determined by a simulation of the complete phase diagram by use of the four-parameter model III (see text).

absolute values of the nonideality parameters the interpretation of these findings has to be made cautiously. If we take the ρ values from Table 2 we would argue that the l.c. phase for both systems behaves nearly ideally. As a consequence we have positive ρ values for the gel phase of the DMPG/DPPC mixture, which means that cluster formation of like molecules is occurring. This is not unexpected, because in many cases miscibility of two unlike components is less in the gel phase than in the l.c. phase. For the DMPA/DPPC mixture negative ρ values are then observed for the gel phase. This indicates the opposite behavior, namely, that the nonideality is such that a kind of complex formation between unlike molecules occurs. This kind of behavior is probably caused by electrostatic effects, i.e., the mutual repulsion of the charged DMPA molecules. It could be enhanced by the ability of DMPA to form hydrogen bonds with the neighboring phosphate groups of a phosphatidylcholine molecule, thereby forming efficient packing by relieving the packing constraints in the headgroup region. That this effect is larger in the gel phase than in the l.c. phase is quite unexpected at first glance. However, one could explain it by assuming that in the l.c. phase hydrogen bonding between headgroups could be reduced because of the expansion in the plane of the bilayer. Likewise the electrostatic repulsive effects decrease in the l.c. phase because of larger separation of the DMPA headgroups.

If we assume positive ρ values for the gel phase, i.e., cluster formation, we would get more positive ρ values for the l.c. phase. This would mean that the nonideality increases with higher temperature in the more disordered phase, and we think that this is relatively unlikely. Therefore, we are certain that the high ρ values and the appearance of a phase diagram with an upper azeotropic point found by simulating the phase diagram based on the empirical $T(-)$ and $T(+)$ values (see Table 2 and Fig. 11) are artifacts that are due to incorrect determination of the phase boundaries.

SUMMARY AND CONCLUSIONS

We have presented new approaches for the simulation of heat-capacity curves and phase diagrams of pseudobinary phospholipid mixtures. We simulated the heat-capacity curves by using the usual two-parameter model for symmetric nonideal mixing in the gel and the l.c. phases. The limited cooperativity of the phase transition was incorporated into the simulation by convolution of the theoretical heat-capacity curves with a broadening function that uses a simple two-state transition model with a van't Hoff enthalpy ΔH_{vH} as an adjustable parameter. This is equivalent to changing the cooperative unit size n.

Analysis of heat-capacity curves of two different lipid mixtures showed that the cooperative unit size decreases drastically for mixtures in the mole fraction range 0.2–0.8. The nonideality parameters obtained from the simulations of the heat-capacity curves were found to be a function of composition of the mixture. This led to the conclusion that for simulation of the coexistence lines of the phase diagram a model using nonsymmetric, nonideal mixing for both phases must give better fits.

Comparison of simulated phase diagrams by use of four different mixing models clearly showed that the four-parameter model mentioned above indeed gives the best fits. Depending on the type of mixing behavior, the analysis of phase diagrams calculated from empirically corrected temperatures for the coexistence lines can give unlikely results for the nonideality parameters.

A major problem in the simulation of phase diagrams is that the phase boundaries change only little when the nonideality parameters are varied, as long as the difference between these parameters for the gel and the l.c. phases remains constant. Therefore, the absolute ρ values are relatively unreliable and should not be interpreted extensively.

For both mixtures shown as examples, nonsymmetric, nonideal mixing was observed. For the system DMPG/DPPC the difference $\Delta\rho = \rho_l - \rho_g$ was found to be negative, whereas for DMPA/DPPC the $\Delta\rho$ value was positive. The latter result is quite unusual and was tentatively

interpreted as being due to complex formation of unlike molecules in the gel phase.

The simulation approach presented here has been successfully tested for a variety of pseudobinary lipid mixtures and has been extended for systems with miscibility gaps in the gel phase. The results of these simulations will be presented in later publications.

This research was supported by grants from the Deutsche Forschungsgemeinschaft (Bl-182/7-2) and from the Fonds der Chemischen Industrie.

REFERENCES

Blume, A. 1988. Applications of calorimetry to lipid model membranes. *In* Physical Properties of Biological Membranes and Their Functional Implications. C. Hidalgo, editor. Plenum Publishing Corporation, New York. 71–121.

Blume, A. 1991. Biological calorimetry: membranes. *Thermochim. Acta.* 193:299–347.

Brumbaugh, E. E., and C. Huang. 1992. Parameter estimation in binary mixtures of phospholipids. *Methods Enzymol.* 210:521–539.

Brumbaugh, E. E., M. L. Johnson, and C. Huang. 1990. Non-linear squares analysis of phase diagrams for non-ideal binary mixtures of phospholipids. *Chem. Phys. Lipids.* 52:69–79.

Cevc, G. 1993. Phospholipids Handbook. Marcel Dekker, New York.

Cevc, G., and D. Marsh. 1987. Phospholipid Bilayers. Physical Principles and Models. John Wiley & Son, New York.

Cheng, W. H. 1980. A theoretical description of phase diagrams for nonideal lipid mixtures. *Biochim. Biophys. Acta.* 600:358–366.

Chernik, G. G. 1995. Phase equilibria in phospholipid-water systems. *Adv. Coll. Interf. Sci.* 61:65–129.

Faunt, L. M., and M. L. Johnson. 1992. Parameter estimation by least-squares methods. *Methods Enzymol.* 210:340–356.

Glaser, M. 1993. Lipid domains in biological membranes. *Curr. Opin. Struct. Biol.* 3:475–481.

Gruenewald, B., S. Stankovski, and A. Blume. 1979. Curvature influence on the cooperativity and the phase transition enthalpy of lecithin vesicles. *FEBS Lett.* 102:227–229.

Guggenheim, E. A. 1944. Statistical thermodynamics of mixtures with zero energies of mixing. *Proc. R. Soc. London.* 203:213–212.

Hildebrandt, H. 1929. Solubility (XII). Regular solutions. *J. Am. Chem. Soc.* 51:66–80.

Hill, T. L. 1960. An Introduction to Statistical Thermodynamics. Addison-Wesley, Reading, MA.

Inoue, T., T. Tasaka, and R. Shimozawa. 1992. Miscibility of binary phospholipid mixtures under hydrated and unhydrated conditions. I. Phosphatidic acids with different acyl chain length. *Chem. Phys. Lipids.* 63:203–212.

Ipsen, J. H., and O. G. Mouritsen. 1988. Modelling the phase equilibria in two-component membranes of phospholipids with different acyl-chain lengths. *Biochim. Biophys. Acta.* 944:121–134.

Lee, A. G. 1977. Lipid phase transitions and phase diagrams. Part 2. *Biochim. Biophys. Acta.* 472:285–344.

Mabrey, S., and J. M. Sturtevant. 1976. Investigation of phase transitions of lipids and lipid mixtures by high sensitivity differential scanning calorimetry. *Biochemistry.* 73:3862–3866.

Nibu, Y., T. Inoue, and I. Motoda. 1995. Effect of headgroup type on the miscibility of homologous phospholipids with different acyl chain lengths in hydrated bilayer. *Biophys. Chem.* 56:273–280.

Press, W. H., B. B. Flannery, S. A. Teukolsky, and W. T. Vetterling. 1986. Numerical Recipes, 2nd ed. Cambridge University Press, Cambridge.

Prausnitz, J. M., R. N. Lichtenthaler, and E. Gomes de Azevedo. 1986. Molecular Thermodynamics of Fluid-Phase Equilibria, 2nd ed. Prentice-Hall, Englewood Cliffs, NJ.

Small, D. M. 1986. The Physical Chemistry of Lipids. Handbook of Lipid Research, Vol. 4. D. J. Hanahan, editor. Plenum Publishing Company, New York.

Sugár, I. P. 1987. Cooperativity and classification of phase aransitions. Application to one- and two-component phospholipid membranes. *J. Phys. Chem.* 91:95–101.

Tenchov, B. G. 1985. Nonuniform lipid distribution in membranes. *Prog. Surf. Sci.* 20:273–340.

von Dreele, P. H. 1978. Estimation of lateral species separation from phase transitions in nonideal two-dimensional lipid mixtures. *Biochemistry.* 19:3939–3943.